Benthic nitrite exchanges in the Seine River (France) An early diagenetic modeling analysis

Zahra Akbarzadeh, Anniet M Laverman, Fereidoun Rezanezhad, Mélanie Raimonet, Eric Viollier, Babak Shafei, Philippe van Cappellen

Science of the Total Environment 628–629 (2018) 580–593

Contents lists available at ScienceDirect

Science of the Total Environment

journal homepage: www.elsevier.com/locate/scitotenv

Benthic nitrite exchanges in the Seine River (France): An early diagenetic modeling analysis

Zahra Akbarzadeh [a,*], Anniet M. Laverman [b], Fereidoun Rezanezhad [a], Mélanie Raimonet [c], Eric Viollier [d], Babak Shafei [e], Philippe Van Cappellen [a]

[a] Ecohydrology Research Group, Water Institute and Department of Earth and Environmental Sciences, University of Waterloo, Canada
[b] UMR 6553 Ecobio, CNRS and Université Rennes 1, Rennes, France
[c] UMR 7619 METIS, Université Pierre et Marie Curie, Paris 6, Sorbonne Universités, Paris, France
[d] Laboratoire de Géochimie des Eaux, UMR 7154, Université Paris Diderot, Paris 7 and Institut de Physique du Globe (IPGP), Paris, France
[e] AquaNRG Consulting Inc., Houston, TX, United States

HIGHLIGHTS

- Elevated concentrations of nitrite (NO_2^-) are observed in the Seine River.
- Sediment cores were collected upstream and downstream of Paris's largest WWTP.
- Benthic fluxes of NO_2^-, NO_3^- and NH_4^+ were measured in core incubations.
- Pore water data and benthic fluxes were analyzed with a reactive transport model.
- Sediments act as source or sink of nitrite, depending on sampling location and time.

GRAPHICAL ABSTRACT

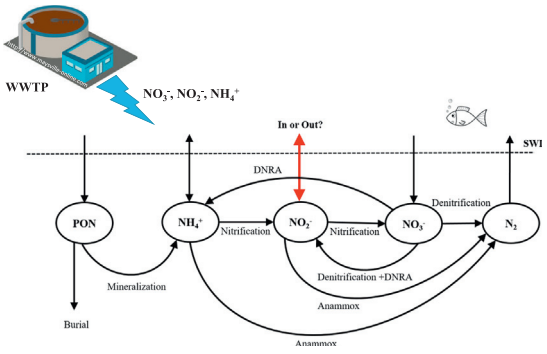

ARTICLE INFO

Article history:
Received 30 October 2017
Received in revised form 10 January 2018
Accepted 30 January 2018
Available online 20 February 2018

Editor: Daniel Wunderlin

Keywords:
Nitrite
River sediments
Seine
Reactive transport modeling
Benthic exchanges
Denitrification
Nitrification
DNRA
Anammox

ABSTRACT

Nitrite is a toxic intermediate compound in the nitrogen (N) cycle. Elevated concentrations of nitrite have been observed in the Seine River, raising questions about its sources and fate. Here, we assess the role of bottom sediments as potential sources or sinks of nitrite along the river continuum. Sediment cores were collected from two depocenters, one located upstream, the other downstream, from the largest wastewater treatment plant (WWTP) servicing the conurbation of Paris. Pore water profiles of oxygen, nitrate, nitrite and ammonium were measured. Ammonium, nitrate and nitrite fluxes across the sediment-water interface (SWI) were determined in separate core incubation experiments. The data were interpreted with a one-dimensional, multi-component reactive transport model, which accounts for the production and consumption of nitrite through nitrification, denitrification, anammox and dissimilatory nitrate reduction to ammonium (DNRA). In all core incubation experiments, nitrate uptake by the sediments was observed, indicative of high rates of denitrification. In contrast, for both sampling locations, the sediments in cores collected in August 2012 acted as sinks for nitrite, but those collected in October 2013 released nitrite to the overlying water. The model results suggest that the first step of nitrification generated most pore water nitrite at the two locations. While nitrification was also the main pathway consuming nitrite in the sediments upstream of the WWTP, anammox dominated nitrite removal at the downstream site. Sensitivity analyses indicated that the magnitude and direction of the benthic nitrite fluxes most strongly depend on bottom water oxygenation and the deposition flux of labile organic matter.

* Corresponding author at: Ecohydrology Research Group, University of Waterloo, 200 University Avenue West, Waterloo, Ontario N2L 3G1, Canada.
E-mail address: zakbarza@uwaterloo.ca (Z. Akbarzadeh).

https://doi.org/10.1016/j.scitotenv.2018.01.319

1. Introduction

Humans have greatly modified the nitrogen (N) cycle, nearly doubling the inputs of bioavailable nitrogen to the environment (Gruber and Galloway, 2008). Excess nitrogen negatively impacts human and ecosystem health, causing eutrophication of aquatic ecosystems, decreasing air quality and contaminating drinking water supplies (Driscoll et al., 2003; Erisman et al., 2013; Ndegwa et al., 2008). The application of N-containing fertilizers and human wastewater release have been linked to the expansion of hypoxic and anoxic conditions in aquatic systems (Diaz and Rosenberg, 2008; Rabalais et al., 2010), while enhanced microbial nitrification and denitrification causes emission of nitrous oxide (N_2O), an important greenhouse gas (Crutzen et al., 2007).

Nitrate (NO_3^-) and nitrous oxide (N_2O) have received most attention as N contaminants. Strict nitrate water quality standards are in place in most developed countries (Oenema et al., 2011), while interest in N_2O emissions stems from concerns about accelerating climate change (e.g. Clough et al., 2006; Beaulieu et al., 2007; Rosamond et al., 2012). In comparison, relatively little research has been done on the intermediate species nitrite (NO_2^-). High nitrite concentrations in drinking water can cause serious illness in infants; shortness of breath and blue baby syndrome are some of the associated symptoms (Knobeloch et al., 2000). The maximum level of nitrite for drinking water set by the US Environmental Protection Agency is 1 ppm. Nitrite is also toxic to aquatic life (Cowling et al., 1998; Philips et al., 2002): according to the EU Water Framework Directive, the nitrite limit for good environmental status is 0.09 mg N-NO_2^- L^{-1}.

Nitrite is a reactive intermediate produced and consumed in several redox pathways of the N cycle (Kelso et al., 1997; Mordy et al., 2010). It is produced during the first steps of nitrification and denitrification from ammonium (NH_4^+) and nitrate (NO_3^-), respectively. Under oxic conditions, nitrite oxidizers consume NO_2^- producing nitrate as part of the overall nitrification process. Under reducing conditions, nitrite can be transformed to N_2 gas during denitrification or anammox, or to ammonium via dissimilatory nitrate reduction to ammonium (DNRA). In addition to biotic transformations, nitrite is chemically reactive (Udert et al., 2005). Thus, in general, nitrite concentrations in the environment are expected to be negligible. Nonetheless, accumulation of nitrite has been observed in rivers and streams. In particular, relatively high nitrite concentrations have been reported in various urbanized rivers, for instance the Lahn River in Germany (von der Wiesche and Wetzel, 1998), rivers of Northern Ireland (Kelso et al., 1997), and the Seine River in France (Garnier et al., 2006; Raimonet et al., 2015; Raimonet et al., 2017).

The Seine River receives large N inputs from diffuse agricultural and urban sources, as well as point sources, primarily waste water treatment plant (WWTP) discharges (Cébron and Garnier, 2005; Naeher et al., 2015; Raimonet et al., 2015; Raimonet et al., 2017). Downstream of the metropolitan area of Paris, the effluents from a very large WWTP, known by its acronym SAV (daily capacity of 1.7 M m^3), greatly impact the river water quality (Vilmin et al., 2014). Nitrogen pollution in the past was dominated by ammonium, resulting in nitrification and even anoxia in the water column (Cébron and Garnier, 2005; Chesterikoff et al., 1992; Garban et al., 1995). Upgrades to the SAV WWTP, with the introduction of treatment by nitrification and denitrification in 2007 and 2011, respectively, considerably decreased N loading to the river: ammonium discharges dropped from 58 ± 22 to 12 ± 17 t N d^{-1} (Aissa-Grouz et al., 2015). Nitrate concentrations in the river have remained elevated, however, mainly because of agricultural activity in the surrounding area. In addition, even after the improvements, nitrite concentrations in the outflow of the WWTP have remained above European water quality standards (Raimonet et al., 2017).

With an estimated daily loading of around 2.4 ± 2 tonnes NO_2-N (Aissa-Grouz et al., 2015), the WWTP is a major source of nitrite to the Seine River (Garnier et al., 2006; Raimonet et al., 2015). Surprisingly, elevated concentrations of nitrite persist for over 300 km downstream of Paris, despite fully oxic conditions along the river channel (Aissa-Grouz et al., 2015). Possible explanations include the sustained production of nitrite in the water column (Raimonet et al., 2015), or a continuous efflux of nitrite from streambed sediments. Benthic processes are known to have a significant impact on the water quality of aquatic systems in general (Han et al., 2014; Paraska et al., 2014; Thouvenot et al., 2007), and on the cycling of nitrogen in particular (Han et al., 2014). Fixed nitrogen is removed by sediments via permanent burial of organic nitrogen and clay-bound ammonium, as well as through denitrification or anammox, which return dinitrogen gas to the atmosphere. Alternatively, dissolved inorganic nitrogen species can be recycled to the water column following mineralization of deposited organic matter (Thamdrup and Dalsgaard, 2008).

Here, we present a preliminary assessment of the potential role of benthic nitrite exchanges in the Seine River: pore water and benthic flux measurements on sediments collected upstream and downstream of the SAV WWTP are analyzed quantitatively by developing and applying an early diagenetic model that includes a comprehensive representation of the benthic N cycle. Early diagenetic models simulate the coupled transport and transformation processes that affect the chemical species of interest below the sediment-water interface (SWI) (Boudreau, 1996). While these reactive transport models have been frequently used to interpret multicomponent data sets collected in marine and lacustrine sediments, applications to riverbed sediments remain limited. Paraska et al. (2014), who reviewed 83 early diagenetic modeling studies published since 1996, only report four studies on river sediments (Devallois et al., 2008; Massoudieh et al., 2010; Trinh et al., 2012; Van Den Berg et al., 2000).

Moreover, existing early diagenetic models representing N transformations rarely account for reactive intermediates in general, and nitrite in particular. A limited number of studies have analyzed nitrite pore water profiles using modeling. Stief et al. (2002) and Meyer et al. (2008), for example, measured nitrite pore water profiles in a freshwater mesocosm experiment and an estuarine sediment, respectively. In both studies, an inverse reaction-transport model was used to extract the depth distributions of nitrite production and consumption rates. Inverse modeling, however, is unable to predict how the rate distributions change under varying boundary conditions and transport regimes, in contrast to the forward reactive transport modeling used here. Box modeling approaches have also been used to estimate nitrite exchanges between streambed sediments and the overlying river (e.g., Aissa-Grouz et al., 2015; Raimonet et al., 2015; Vilmin et al., 2014), or to simulate nitrite production and consumption in sediments incubation experiments (e.g., Babbin and Ward, 2013). However, because box models do not predict spatial distributions they are not appropriate to analyze pore water profiles. Closest to our modeling approach is that of Dale et al. (2011) who developed a diagenetic model that includes nitrite as a reactive species and represents nitrification, denitrification, DNRA and anammox. This model was applied to a data set from a coastal marine site in the Baltic Sea.

In the present paper, we expand the reaction network for benthic N cycling in an existing early diagenetic computer code in order to explicitly include the reaction pathways producing and consuming nitrite. Reactive transport calculations are then used to interpret a data set

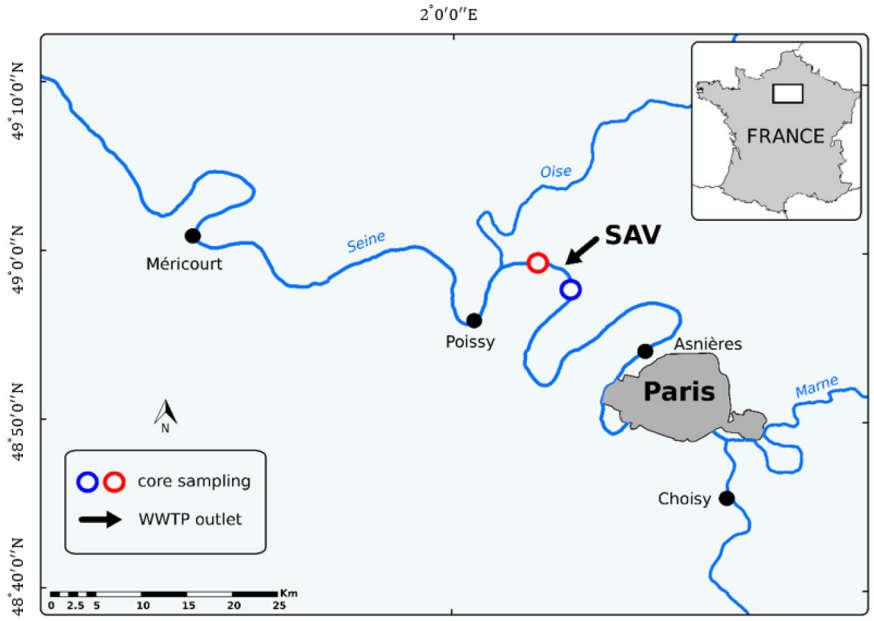

Fig. 1. Locations of the SAV wastewater treatment plant (WWTP) and the upstream (blue circle) and downstream (red circle) core sampling sites. (For interpretation of the references to colour in this figure legend, the reader is referred to the web version of this article.)

comprising pore water profiles and benthic exchange fluxes of nitrate, nitrite and ammonium collected in the Seine River upstream and downstream of the SAV WWTP. Because of the highly dynamic and heterogeneous nature of streambed sediments, we primarily aim to capture the general trends of the measured pore water depth profiles and benthic fluxes. We then use the model as a sensitivity tool to delineate the main controls on benthic exchange fluxes of nitrite.

2. Field sampling and experimental methods

2.1. Seine River

The Seine River is the second longest river in France (776 km). The climate is temperate, with oceanic and semi-continental influences. The mean annual discharge rate of the Seine River at Austerlitz Bridge in Paris is 310 $m^3\ s^{-1}$ (period 1979–2012, Raimonet et al., 2015). The summer river discharge is artificially maintained above 100 $m^3\ s^{-1}$ by water release from dam reservoirs upstream of Paris. Water temperature ranges from 5 °C in winter to 25 °C in summer. The drainage basin of the Seine River is characterized by intense urbanization and agriculture leading to nutrient enrichment, especially by nitrate.

The water quality of the middle reaches of the Seine River is significantly affected by effluents from the largest WWTP in Europe, known by its acronym SAV (>5 million population equivalents) located 70 km downstream of Paris (Fig. 1; Rocher et al., 2015; Vilmin et al., 2015). A recent hydro-ecological modeling study shows that the Seine River downstream of Paris is heterotrophic and that nutrient exchanges across the sediment-water interface (SWI) significantly impact the carbon, nitrogen and phosphorus export fluxes to the Seine River estuary (Vilmin et al., 2015). Weekly measurements of 5-day Biological Oxygen Demand (BOD5) measured on water column samples collected in August 2012 upstream (Bougival) and downstream (Poissy) of SAV WWTP were on average 0.63 and 1.13 mg L^{-1}, respectively. In October 2013, the corresponding average BOD5 values were 1.25 and 1.36 mg L^{-1} (Data from "Vincent Rocher, SIAAP, pers. comm.").

2.2. Sediment coring and pore water extraction

Sediment cores were collected from two sites, one located upstream, the other downstream of the SAV WWTP (Fig. 1), in August 2012 and October 2013 in order to measure vertical pore water concentration profiles of nitrate, nitrite and ammonium. Water temperatures at the sampling sites were higher in August (~23 °C) than in October (~13 °C). At each site, two pre-drilled (and taped) and seven undrilled Plexiglass cores (10–40 cm long; 8.4 cm diameter) were obtained using the UWITEC© piston coring system (Mondsee, Austria). Pore

Table 1
Reaction formulas and rate expressions.

Process	Formula	Rate expression
Aerobic respiration[a]	$(CH_2O)_{org} + y(NH_3)_{org} + z(H_3PO_4)_{org} + O_2 + (2z-y)HCO_3^- \rightarrow \mathbf{yNH_4^+} + zHPO_4^{2-} + (1-y+2z)CO_2 + (1-y+2z)H_2O$	$R1 = k1 \times [POC] \times \frac{[O_2]}{[O_2]+Ko}$
Denitrification	$(CH_2O)_{org} + y(NH_3)_{org} + z(H_3PO_4)_{org} + \mathbf{0.8NO_3^-} \rightarrow \mathbf{0.4\,(1-\alpha-\beta)N_2} + \mathbf{yNH_4^+} + \mathbf{0.8\alpha NO_2^-} + \mathbf{0.4\,\beta N_2O} + zHPO_4^{2-} + (0.8-0.8\alpha+y-2z)\,HCO_3^- + (0.2-y+2z+0.8\alpha)CO_2 + (0.6-y+2z-0.8\alpha-0.4\beta)H_2O + (0.8\alpha-0.4\beta)H_2$	$R2 = k2 \times [POC] \times \frac{[NO_3^-]}{[NO_3^-]+kmno} \times \frac{kin}{[O_2]+Kin} \times \gamma$ Nitrite production: $R3 = 0.8\alpha \times R2$
DNRA	$(CH_2O)_{org} + y(NH_3)_{org} + z(H_3PO_4)_{org} + \mathbf{0.5NO_3^-} \rightarrow \mathbf{((0.5-\delta)+y)NH_4^+} + \mathbf{0.5\delta NO_2^-} + zHPO_4^- + (y-2z)HCO_3^- + (1-y+2z)CO_2 + (0.33-y+2z)H_2O + \delta H_2$	$R5 = k2 \times [POC] \times \frac{[NO_3^-]}{[NO_3^-]+kmno} \times \frac{kin}{[O_2]+Kin} \times (1-\gamma)$ Nitrite production: $R6 = 0.5\delta \times R5$
Anammox	$NH_4^+ + NO_2^- \rightarrow N_2 + 2H_2O$	$R7 = R7_{max} \times \frac{[NH_4^+]}{[NH_4^+]+Km1} \times \frac{[NO_2^-]}{[NO_2^-]+Km2} \times \frac{Kin}{[O_2]+Kin}$
Nitrification (step 1)	$NH_4^+ + 1.5O_2 \rightarrow NO_2^- + H_2O + 2H^+$	$R8 = R8_{max} \times \frac{[NH_4^+]}{[NH_4^+]+Km3} \times \frac{[O_2]}{[O_2]+Km4}$
Nitrification (step 2)	$NO_2^- + 0.5O_2 \rightarrow NO_3^-$	$R9 = R9_{max} \times \frac{[NO_2^-]}{[NO_2^-]+Km5} \times \frac{[O_2]}{[O_2]+Km6}$

[a] y and z are the molar N:C and P:C ratios of the degrading organic matter.

Table 2a
Model parameters.

Parameter	Description	Value	Source[a]
Ko	Half saturation constant of oxygen in aerobic respiration	8 μM	L[b]
Kmno	Half saturation constant of nitrate in denitrification	10 μM	L[b]
Km1	Half saturation constant of ammonium in anammox	5 μM	L[c]
Km2	Half saturation constant of nitrite in anammox	5 μM	L[c]
Km3	Half saturation constant of ammonium in nitrification (step 1)	10 μM	L[d]
Km4	Half saturation constant of oxygen in nitrification (step 1)	15.6 μM	L[d]
Km5	Half saturation constant of nitrite in nitrification (step 2)	10 μM	L[d]
Km6	Half saturation constant of oxygen in nitrification (step 2)	34.4 μM	L[d]
Kin	Coefficient describing inhibition by O_2	8 μM	L[b]
Do2	Molecular diffusion coefficient for oxygen (@20 °C)	651 $cm^{-2}y^{-1}$	L[b]
Dno3	Molecular diffusion coefficient for nitrate (@20 °C)	540 $cm^{-2}y^{-1}$	L[b]
Dno2	Molecular diffusion coefficient for nitrite (@20 °C)	534 $cm^{-2}y^{-1}$	L[e]
Dnh4	Molecular diffusion coefficient for ammonium (@20 °C)	560 $cm^{-2}y^{-1}$	L[e]
γ	Fraction of total nitrate reduction occurring via denitrification	95 (%)	L[f]
∅	Porosity	0.8	E
ω	Burial velocity	0.88 cm y^{-1}	E
α	Nitrite leakage during denitrification	3–5 (%)	CC
β	Nitrous oxide leakage during denitrification	1 (%)	CC
δ	Nitrite leakage during DNRA	3–5 (%)	CC
k1	Degradation rate constant associated with POC1 for August and October	10 y^{-1}	CC
k2	Degradation rate constant associated with POC2 for August and October	1 y^{-1}	CC
C:N	Range of carbon to nitrogen ratio in different pools of organic matter	9.6–21.2	CC

[a] Values obtained from the literature = L; estimated = E; and using a constrained calibration = CC (see Section 3.2).
[b] Van Cappellen and Wang (1995).
[c] Strous et al. (1999).
[d] Raimonet et al. (2015).
[e] Boudreau (1997).
[f] Canavan et al. (2007).

waters were extracted by horizontally inserting Rhizon© samplers (MOM MicroRhizon™ samplers, Ejikelamp, Netherlands) into two replicate sediment cores through the small, pre-drilled holes along the sides of the tubes (1 cm depth intervals from +0.5 cm above to −9.5 cm depth below the SWI). Each Rhizon sampler collected about 2–4 ml filtered pore water directly into a vial. The pore waters were extracted within <5 h after core retrieval. An aliquot of 0.3 ml of each pore water sample was immediately analyzed for NO_2^-, while the remaining sample was stored at −20 °C for later NH_4^+ and NO_3^- analyses.

2.3. Core incubations

Benthic fluxes of nitrate, nitrite and ammonium were measured in August 2012 and October 2013 on triplicate cores collected upstream and downstream of the WWTP. Note that benthic fluxes of nitrate and ammonium were not measured at the downstream site in August 2012. Sediment cores collected in Plexiglass tubes were transported to the laboratory and kept in the dark at 20 °C until the end of the incubations. Incubations started <5 h after core collection. Overlying water was adjusted to 8 cm above the SWI. The bubbling of air at 3–4 cm above the SWI homogenized the overlying water and maintained oxygenated (air) conditions in order to mimic the fully oxic conditions at the SWI (Aissa-Grouz et al., 2015). The dissolved oxygen concentration above the SWI was monitored with an oxygen optode (Pyroscience©), calibrated in O_2 saturated water at the same temperature and salinity as the overlying water using the Firesting Logger software. Incubations ran for 15 h in August 2012, and for one day in October 2013. Periodically, at time intervals ranging between 1 and 10 h, 5 ml of overlying water were collected with a syringe and immediately filtered through a 0.2 μm pore size PVDF filter. A 0.3 ml aliquot of the filtrate was directly analyzed for NO_2^-; the remaining solution was stored at −20 °C for later NH_4^+ and NO_3^- analyses. The net benthic fluxes of NH_4^+, NO_2^- and NO_3^- were calculated from the linear changes in concentration and the known volumes of overlying water and the sediment surface area.

2.4. Analytical methods

Pore water oxygen profiles were measured with Clark-type polarographic microsensors equipped with a built-in reference and an internal guard cathode (Revsbech, 1989). The sensors have an outer tip diameter of 50 or 100 μm (Unisense, Århus, Denmark) and were operated with a motor-driven micromanipulator. The sensor current was measured with a picoamperometer connected to an A-D converter, which transferred the signals to a computer (Revsbech and Jørgensen, 1986). For each site, at least 5 oxygen profiles were recorded on the same core. The microelectrodes were calibrated in O_2 saturated overlying water at 20 °C. The vertical resolution of the measurements was 50–100 μm. The position of the SWI was identified by the sharp break in the O_2 concentration gradient (Sweerts and de Beer, 1989). Oxygen pore water profiles were measured at the upstream and downstream sites in October 2013, but only at the downstream site in August 2012.

Nitrite concentrations were determined by the colorimetric method of Rodier (1984), using a UV/visible spectrophotometer. The method was adapted for microplate analysis to optimize the analysis time and pore water volume (0.3 ml; MDL: 0.1 μM). Ammonium and nitrate concentrations were measured by ionic chromatography (IC, Dionex; MDL: 0.1 μM). Organic carbon and total nitrogen concentrations were measured on air-dried sediment samples from the topmost 8 cm of the October cores at both locations: 2 g aliquots were decarbonated by

Table 2b
Reaction parameters based on model calibration for August 2012 and, in brackets, October 2013.

Process	Upstream	Downstream
	Maximum rate (μmol cm^{-3} yr^{-1})	Maximum rate (μmol cm^{-3} yr^{-1})
Anammox	$R6_{max}$ = 3 (4)	$R6_{max}$ = 14 (15)
Nitrification (step 1)	$R7_{max}$ = 400 (800)	$R7_{max}$ = 80 (225)
Nitrification (step 2)	$R8_{max}$ = 1000 (2000)	$R8_{max}$ = 170 (600)

Table 2c
Parameters obtained by constrained model calibration. The ranges are based on the literature listed with the exception of the C:N ratio in different pools of organic matter.

Parameter	Value	Unit	Range	References
k1	10	y^{-1}	0 − 303	Paraska et al., 2014
k2	1	y^{-1}	0 − 1.1	Paraska et al., 2014
$R6_{max}$	3–15	μmol cm^{-3} yr^{-1}	0.7 − 263	Crowe et al., 2017; Zhu et al., 2013; Yoshinaga et al., 2011
$R7_{max}$, $R8_{max}$	80–2000	μmol cm^{-3} yr^{-1}	0 − 8833	Altmann et al., 2003; Rysgaard et al., 1994; Cooper, 1984
α	3–5	%	0–8	Laverman et al., 2010[a]
β	1	%	0–0.08	Laverman et al., 2010
δ	3–5	%	0–8	Laverman et al., 2010[a]
C:N	9.6–21.2	–	10–31	This study (Section 4.1)

[a] Nitrite production as a percentage of the nitrate reduction rate.

adding 50 ml 1 N HCL (normapur) and, after mixing, kept overnight at 50 °C. The sediments were subsequently washed three times with 50 ml of MilliQ water (50 ml) and centrifuged. The decarbonated and washed sediment samples were then freeze dried and analyzed on an Elemental Analyzer.

3. Early diagenetic modeling

3.1. Conservation equations

An in-house developed, one-dimensional (1D) early diagenetic model was expanded by incorporating a more complete representation of N cycling in sediments. Here, we focus on the newly developed N reaction network; for a description of the original model and examples of applications, the reader is referred to Couture et al. (2010) and Torres et al. (2015). The model is written in MATLAB® and solves the partial differential equations describing mass conservation of the selected pore water solutes and sediment-bound chemical species. The model considers three pools of organic carbon (one most reactive, one less reactive and one unreactive pool), and the following N species: particulate organic N (PON), nitrate (NO_3^-), nitrite (NO_2^-), ammonium (NH_4^+), dissolved nitrous oxide (N_2O) and dissolved nitrogen gas (N_2). Additional solute species included are molecular oxygen (O_2), sulfate (SO_4^{2-}), total sulfide (ΣH_2S), ferrous iron (Fe^{2+}) and methane (CH_4); additional solid species include reactive iron (hydr)oxides ($Fe(OH)_3$), iron monosulfide (FeS) and pyrite (FeS_2).

The reaction stoichiometries and rate expressions describing the N transformation processes included in the model are given in Table 1. Nitrite production during denitrification and DNRA are calculated as adjustable fractions of the corresponding rates of nitrate consumption. These fractions represent the NO_2^- leakage into the environment from cells carrying out nitrate reduction (Richardson et al., 2009; Trimmer et al., 2005). Nitrification is represented as a two-step process with NO_2^- as the intermediate, consistent with the fact that the two steps are catalyzed by two distinct groups of microorganisms (Stein, 2015; Ward, 2013). Monod-type dependencies on substrate concentrations are used to describe the rates of denitrification (organic matter and nitrate), nitrification step 1 (ammonium and oxygen), nitrification step 2 (nitrite and oxygen), anammox (nitrite, ammonium) and DNRA (organic matter and nitrate). Inhibition terms describe the reductions in the rates of denitrification, DNRA and anammox in the presence of dissolved molecular oxygen.

The model accounts for solute transport by molecular diffusion, sediment mixing, advective burial and pore water irrigation, and for solid-bound chemical constituents by advective burial and sediment mixing. The conservation equations describing the distributions of pore water (C_d) and solid-bound (C_s) concentrations are:

$$\frac{\partial(\varnothing C_d)}{\partial t} = D_B\frac{\partial^2(\varnothing C_d)}{\partial x^2} - \varnothing D_s\frac{\partial^2(C_d)}{\partial x^2} - \frac{\partial[\varnothing\omega C_d]}{\partial x} + \varnothing\alpha(C_{d0} - C_d) + \varnothing\sum R_d \quad (1)$$

$$\frac{\partial[(1-\varnothing)\rho C_s]}{\partial t} = D_B\frac{\partial^2[(1-\varnothing)\rho C_s]}{\partial x^2} - \frac{\partial[(1-\varnothing)\omega\rho C_s]}{\partial x} + (1-\varnothing)\rho\sum R_s \quad (2)$$

where ϕ is sediment porosity, α the pore water irrigation coefficient (yr^{-1}), ω the sediment burial velocity (cm yr^{-1}), D_s and D_B the molecular diffusion and sediment mixing coefficients, respectively (cm^2 yr^{-1}), and ρ the sediment dry density (g cm^{-3}). In the absence of time series data, only steady state results are reported here, that is, the conservation Eqs. (1) and (2) were solved with the LHS set equal to zero.

The rates R_d and R_s, for solutes and solids respectively, are positive when the corresponding chemical constituent is produced, and negative when consumed. For example, for nitrite, nitrate and ammonium the rate expressions are (see Table 1 for the numbering of the rates):

$$\sum R(NO_2^-) = 0.8R_3 + 0.5R_6 + R_8 - R_7 - R_9 \quad (3)$$

$$\sum R(NO_3^-) = R_9 - 0.8R_2 - 0.5R_5 \quad (4)$$

$$\sum R(NH_4^+) = yR_1 + yR_2 + ((0.5-\delta)+y)R_5 - R_7 - R_8 + R_{Rest} \quad (5)$$

Table 3
Upper boundary conditions at locations upstream and downstream of the SAV WWTP in August 2012 and October 2013.

Variables	Upstream		Downstream		Units	References
	August 2012	October 2013	August 2012	October 2013		
O_2	300	233	250	222	μM	Measurement
NO_2^-	5.4	3.5	15	6.6	μM	Measurement
NO_3^-	252	270	345	415	μM	Measurement
NH_4^+	5.3	25	6.7	70	μM	Measurement
SO_4^{2-}	513	585	513	585	μM	Model calibration
Fe^{2+}	0	0	0	0	μM	Assumed
POC1	1700	2700	2500	3800	μmol cm^{-2} y^{-1}	Model calibration
POC2	600	800	600	800	μmol cm^{-2} y^{-1}	Model calibration
POC3	500	500	500	500	μmol cm^{-2} y^{-1}	Model calibration
$Fe(OH)_3$	50	50	50	50	μmol cm^{-2} y^{-1}	Model calibration
H_2S	0	0	0	0	μmol cm^{-2} y^{-1}	Assumed
FeS	0	0	0	0	μmol cm^{-2} y^{-1}	Assumed
FeS_2	0	0	0	0	μmol cm^{-2} y^{-1}	Assumed

where R_{Rest} is the sum of the rates of ammonium release during the degradation of organic matter by dissimilatory iron(III) reduction, sulfate reduction and methanogenesis.

3.2. Parameter values and boundary conditions

The reaction and transport parameter values listed in Tables 2a, 2b and 2c were obtained following a procedure common in early diagenetic modeling (e.g., Wang and Van Cappellen, 1996; Dale et al., 2008, 2011; Couture et al., 2010; Krumins et al., 2013; Torres et al., 2015). Where possible, parameter values were retrieved directly from the literature (L parameters in Table 2a) or else estimated a priori (E parameters in Table 2a). An example of the latter is the sediment porosity, which was not measured and therefore assigned a typical value of 0.8. The remaining model parameters were then adjusted by trial and error to yield global fits of the model to the combined pore water geochemistry and benthic flux data sets. For the majority of these fitted parameters, the values were only allowed to vary within published ranges; these parameters are labeled CC (for constrained calibration).

Aqueous concentrations measured in the overlying water were assigned as upper boundary conditions for the pore water species. For all solid-bound species the deposition fluxes at the SWI were imposed (Table 3). Because the oxygen penetration depth depends primarily on the supply of the most reactive pool of sedimentary organic carbon (POC1), it was used to estimate the POC1 deposition flux. The deposition flux of the less reactive organic carbon pool (POC2) was then adjusted to best reproduce the pore water profiles of nitrate and ammonium. The resulting deposition fluxes of POC1 at the downstream site were higher than at the upstream site (Table 3), likely due to the deposition of organic matter released by the wastewater treatment plant. Given that the river was fully oxygenated, the deposition fluxes of FeS and FeS_2 were assumed equal to zero, while those of reactive ferric iron oxyhydroxides, represented as $Fe(OH)_3$, were adjusted to best fit the lower parts of the ammonium profiles. As lower boundaries, zero concentration gradients were imposed for all the chemical species.

In the early diagenetic literature, infaunal activity is usually assumed to be the main cause of pore water irrigation and sediment mixing. Infaunal activity in the Seine river sediments is supported by the observation of shells and burrows in the upper 20 cm of sediment at both sites. However, fitting of the measured pore water profiles and benthic exchange fluxes yielded values of D_B at the SWI of up to 600 $cm^2\ yr^{-1}$ (Tables 4a and 4b), that is values exceeding those typically ascribed to bioturbation (Boudreau, 1997; Lecroart et al., 2007). Similarly, the inferred pore water irrigation coefficients, α, in the upper sediment layers tend to be on the high side of values reported for infaunal activity (Meile and Van Cappellen, 2003). The likely explanation is that in high-energy systems, such as estuaries and rivers, the top sediment layer is continuously mixed physically by the overlying water, which in the model formulation translates in high α and D_B values for the topmost, submillimeter sediment layer (Laverman et al., 2007). Below this surficial layer, α and D_B drop off very rapidly to values that are in line with values reported for infaunal bioirrigation and bioturbation.

4. Results and discussion

4.1. Sediment respiration

The organic carbon concentrations measured in October 2013 in the upstream cores range from 3.8 to 6.9 wt%. At the downstream site, the concentrations are markedly higher, varying between 6.6 and 11.4 wt %. The sediment nitrogen concentrations are similarly higher at the downstream site (0.4–0.9 wt%) than at the upstream site (0.1–0.3 wt%). The organic matter in the downstream cores is also enriched in N (molar C:N = 10–15) compared to the upstream cores (molar C:N = 19–31). Higher organic C loadings at the downstream site are consistent with the reported BOD5 values (see Section 2.1. *Seine River*), which imply higher rates of water column respiration downstream of the WWTP. The BOD5 values also suggest higher respiration rates in October compared to August. The shallow pore water oxygen penetration depths (2–3 mm) provide further evidence of high respiratory activity in the river sediments (Fig. 1S).

Table 4a
Sediment mixing and pore water irrigation coefficients in August 2012.

Depth (x)	Downstream	
	Sediment mixing $cm^2\ yr^{-1}$	Pore water irrigation yr^{-1}
$x < 0.1$ cm	$D_B = 300$	$\alpha = 200$
$0.1 < x < 4$ cm	$D_B = 100$	$\alpha = 50$
$4 < x < 20$ cm	$D_B = 5$	$\alpha = 20$
Depth (x)	**Upstream**	
	Sediment mixing $cm^2\ yr^{-1}$	Pore water irrigation yr^{-1}
$x < 0.1$ cm	$D_B = 150$	$\alpha = 200$
$0.1 < x < 4$ cm	$D_B = 150$	$\alpha = 50$
$4 < x < 20$ cm	$D_B = 5$	$\alpha = 10$

The model-derived POC1 deposition fluxes (Table 3), the depth-integrated rates of organic C oxidation, and the benthic O_2 consumption rates (Table 5) are in line with the above observations. They confirm that sediment respiration is higher downstream than upstream of the WWTP, and higher in October than in August. The total sediment O_2 consumption rates vary between 708 and 1665 μmol $O_2\ cm^{-2}\ yr^{-1}$, which is consistent with sediment O_2 consumption rates typically reported for freshwater sediments (Rong et al., 2016; Tomaszek and Czerwieniec, 2003). According to the model calculations, between 75 and 92% of the total sediment O_2 consumption is due to oxygen respiration coupled to organic matter oxidation, with nitrification being the next most important pathway consuming O_2. The contribution of nitrification (step 1 plus step 2) to O_2 reduction, however, is significantly larger at the upstream (22–25%) site, compared to the downstream site (8–12%). The inferred dominant roles of organic matter oxidation and nitrification in benthic O_2 uptake agrees with previous studies (Canavan et al., 2006; Clevinger et al., 2014; Hall and Jeffries, 1984).

4.2. Pore water N profiles

The impact of the WWTP is also seen in the water column chemistry: the bottom water concentrations of nitrate, nitrite and ammonium are all higher at the downstream site (Table 3). For example, the downstream bottom water nitrite concentrations are in the range of 10–15 μM, compared to 3–5 μM upstream concentrations. Depth profiles of the various pore water N species are shown in Fig. 2 for August and Fig. 3 for October. The profiles measured on the duplicate cores collected at the two sites exhibit significant variability, in particular for nitrite and

Table 4b
Sediment mixing and pore water irrigation coefficients in October 2013.

Depth (x)	Downstream	
	Sediment mixing $cm^2\ yr^{-1}$	Pore water irrigation yr^{-1}
$x < 0.1$ cm	$D_B = 600$	$\alpha = 300$
$0.1 < x < 2$ cm	$D_B = 300$	$\alpha = 100$
$2 < x < 20$ cm	$D_B = 10$	$\alpha = 15$
Depth (x)	**Upstream**	
	Sediment mixing $cm^2\ yr^{-1}$	Pore water irrigation yr^{-1}
$x < 0.1$ cm	$D_B = 500$	$\alpha = 300$
$0.1 < x < 3$ cm	$D_B = 200$	$\alpha = 200$
$3 < x < 20$ cm	$D_B = 10$	$\alpha = 10$

Table 5
Benthic O_2 consumption rates; values in brackets correspond to percentages of the total O_2 consumption rates.

Reaction rate	Upstream		Downstream	
(μmol O_2 cm^{-2} yr^{-1})	August 2012	October 2013	August 2012	October 2013
Organic matter oxidation with O_2	708 (75)	1230 (78)	1305 (88)	1665 (92)
Nitrification step 1	180 (19)	271 (17)	143 (10)	126 (7)
Nitrification step 2	60 (6)	82 (5)	23(2)	25 (1)
Fe oxidation by O_2	0.6 (<0.5)	0.002 (<0.5)	0.04 (<0.5)	0.007 (<0.5)
H_2S oxidation by O_2	0.4 (<0.5)	0.2 (<0.5)	4 (<0.5)	0.9 (<0.5)
Total	949 (100)	1583 (100)	1475 (100)	1817 (100)

ammonium. Given the high spatial heterogeneity, the model fits therefore only aim to capture the general trends of the concentration depth profiles. Irrespective of site and sampling time, the nitrate concentrations drop to zero within the upper 3–4 cm. Similar nitrate profiles have been observed in earlier work on estuarine and freshwater sediments (Meyer et al., 2005; Laverman et al., 2007). The steep nitrate pore water gradients reflect the very high rates of denitrification in the uppermost centimeters of sediments in these environments. The ammonium pore water profiles show increasing trends with depth, reaching concentrations of up to 2 mM in October. According to the model results, most pore water ammonium is produced from the breakdown of organic matter (Figs. 2 and 3).

Compared to nitrate, far fewer nitrite pore water profiles have been published, though nitrite has been shown to be present in sediment pore waters (Stief et al., 2002; Meyer et al., 2005) and in river water (Kelso et al., 1997; von der Wiesche and Wetzel, 1998; Raimonet et al., 2015). The nitrite profiles measured in the sediments collected at the upstream site shows a subsurface peak at 3–4 cm depth. Similar subsurface peaks have previously been observed in estuarine and mangrove sediments using NOx microsensors (Meyer et al., 2008, 2005). At the downstream site, the highest nitrite concentrations are found right at the SWI. The nitrite profiles reflect the depth distributions of the processes that consume and produce nitrite, primarily nitrification, denitrification and anammox (see also Stief et al., 2002; Meyer et al.,

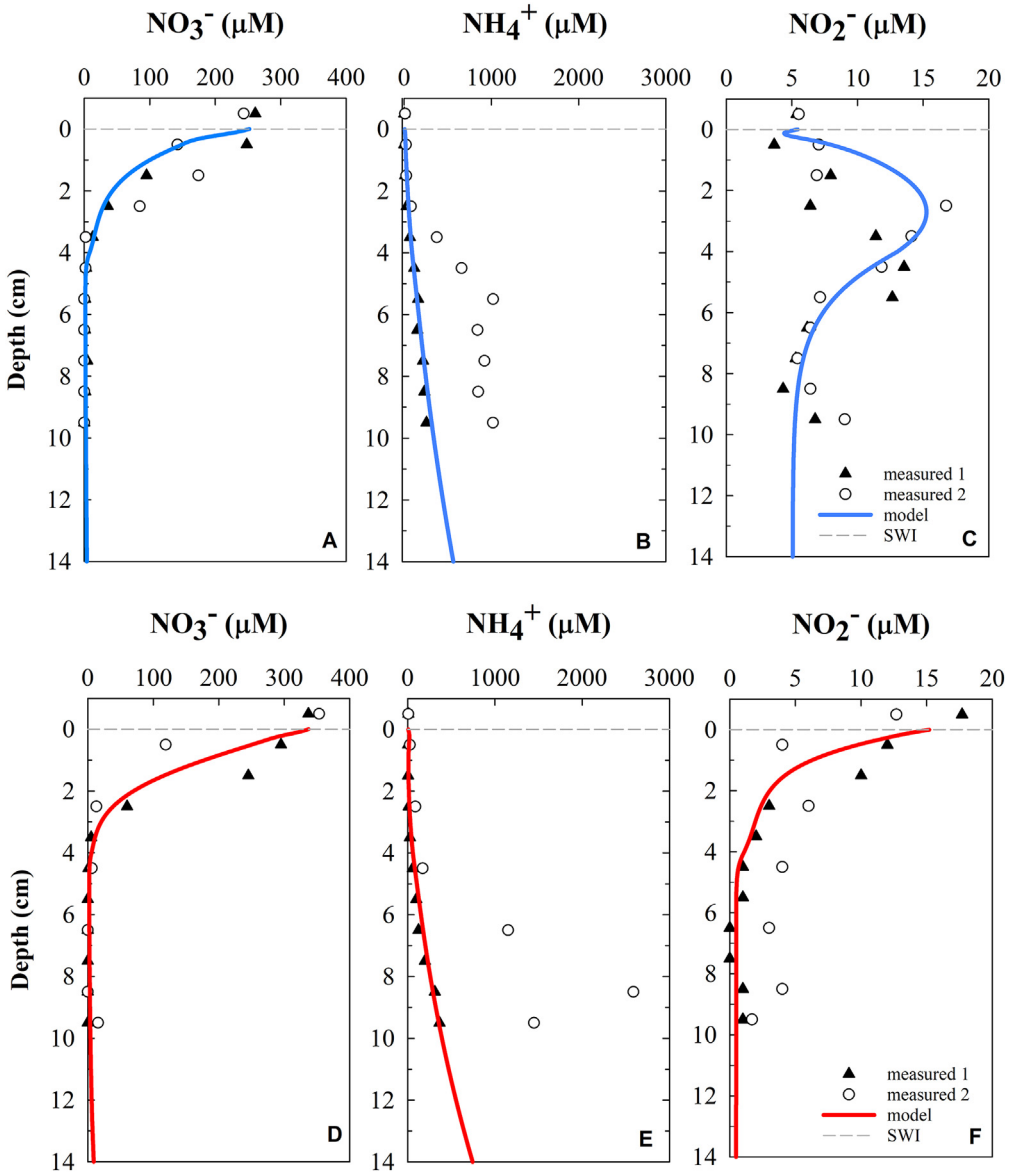

Fig. 2. Measured and modeled pore water profiles of nitrogen species upstream (A, B, C) and downstream (D, E, F) of the SAV wastewater treatment plant in August 2012.

2005). According to the model simulations, the absence of a pronounced nitrite peak at the downstream site is the result of the much higher rates of aerobic carbon oxidation right below the SWI and, in turn, the lower nitrification rates in the top centimeters of sediment. Also at the downstream site, higher rates of anammox in the presence of ammonium and nitrite affect the shape of nitrite profiles at the SWI. The generally low nitrite levels in the bottom portions of the cores are attributed to consumption by anammox.

4.3. Benthic N cycling: reaction rates

Depth-integrated rates estimated with the model are provided in Table 6 and Figs. 4 and 5. The figures schematically illustrate the mechanistic insights that can be gained by applying the reactive model to the pore water geochemistry and core incubation data. In particular, they show the close coupling between the various N transformation processes and benthic exchanges. As expected, denitrification is predicted to be the main N transformation pathway in the sediments, with most of the nitrate consumed by the denitrifiers supplied by influx from the overlying water, although nitrification also contributes 19–21% of the pore water nitrate supply at the upstream site. The depth-integrated rates of denitrification are much higher in October than in August. For nitrification, the largest differences in depth-integrated rates are observed between the upstream and downstream sites, because the lower deposition of highly reactive organic matter (POC1, Table 3) at the upstream site leaves a greater fraction of pore water O_2 available for the aerobic oxidation of ammonium and nitrite.

The modeled rates of denitrification for the Seine River sediments fall in the range 497–1248 μmol cm^{-2} yr^{-1}. These rates are consistent with previous studies on Seine sediments (Table 6). Billen et al. (2007) report a range of benthic denitrification rates between 60 and 2500 μmol cm^{-2} yr^{-1} based on a large scale survey of direct measurements along the Seine drainage network, while Thouvenot-Korppoo et al. (2009) estimate mean rates in the range 125–625 μmol cm^{-2} yr^{-1} averaged over a stretch of the Seine River from 80 km upstream to 100 km downstream of Paris. The very high rates of denitrification observed in the Seine River sediments are characteristic of river systems receiving large anthropogenic inputs of nitrogen and organic carbon. For comparison, Table 1S gives denitrification rates measured in sediments of other rivers and river impoundments.

The depth-integrated rates of DNRA are in the range of 16–41 μmol cm^{-2} yr^{-1}. Thus, DNRA accounts only for about 3% of the total rates of nitrate reduction in the sediments. As for denitrification, the rates of DNRA are higher in October than in August, due to the higher supply of

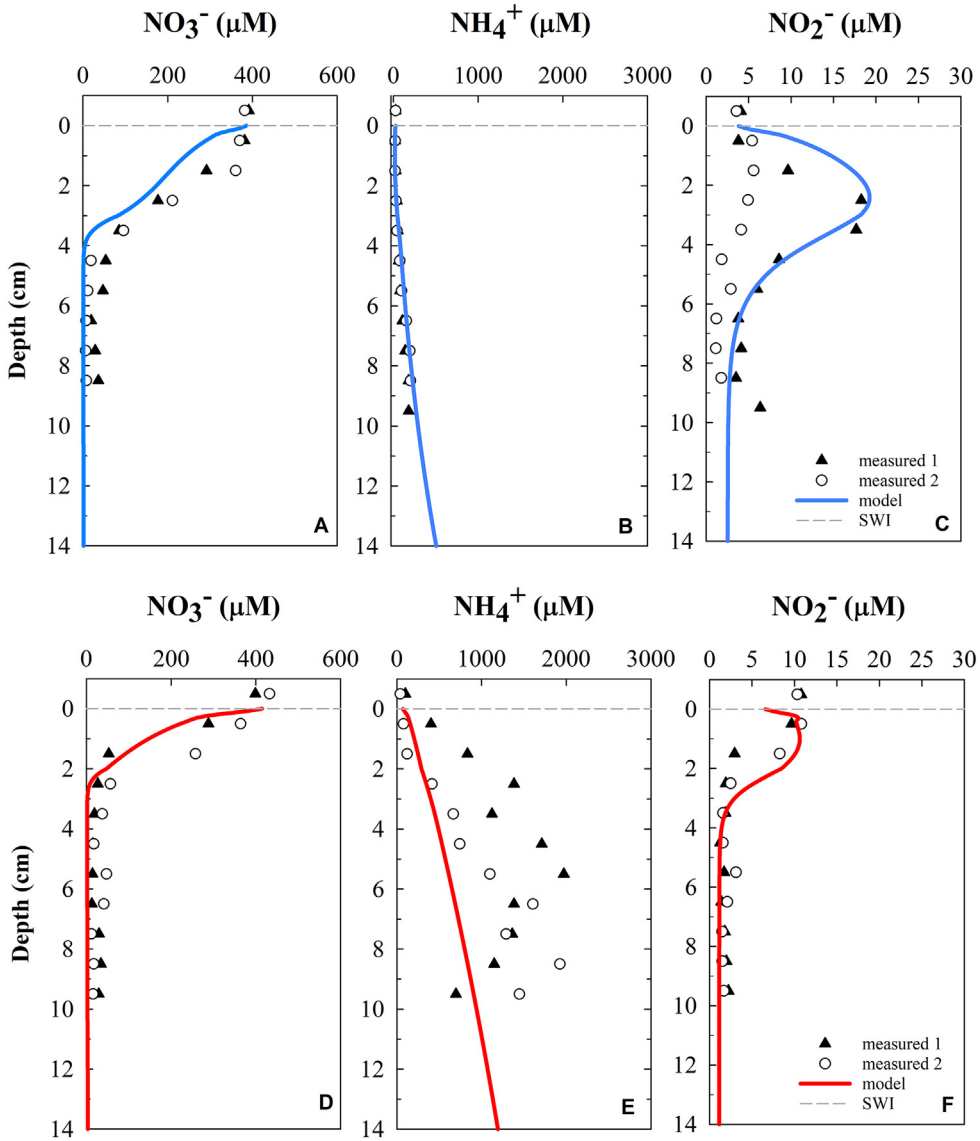

Fig. 3. Measured and modeled pore water profiles of nitrogen species upstream (A, B, C) and downstream (D, E, F) of the SAV wastewater treatment plant in October 2013.

Table 6
Depth integrated rates (μmol N cm^{-2} yr^{-1}) for different processes upstream and downstream of the SAV WWTP in August 2012 and October 2013.

Reaction	Upstream		Downstream		Range in literature	References
	August 2012	October 2013	August 2012	October 2013		
Nitrification (step1)	120	191	95	84	<5000	[1], [2], [3], [4], [5]
Denitrification	554	829	497	1248	<13,850	[5], [6], [7], [8], [9], [10], [11], [12]
DNRA	18	27	16	41	<219	[13], [14], [15], [16]
Anammox	33	33	78	73	0.1 — 720	[17], [18], [19]

[1]: (Pauer, 2000), [2]: (Strauss et al., 2004), [3]: (Stief and de Beer, 2006), [4]: (Meyer et al., 2008), [5]: (Keffala et al., 2011), [6]: (Laursen and Seitzinger, 2002), [7]: (Canavan et al., 2006), [8]: (Tomaszek and Czerwieniec, 2000), [9]: (Seitzinger, 1988), [10]: (García-Ruiz et al., 1998), [11]: (Thouvenot-Korppoo et al., 2009), [12]: (Billen et al., 2007), [13]: (Gardner and McCarthy, 2009), [14]: (Dale et al., 2011), [15]; (McCarthy et al., 2007), [16]: (Gardner et al., 2006), [17]: (Zhao et al., 2013), [18]: (Shen et al., 2015), [19]: (Wang et al., 2013).

reactive organic matter in October. The modeled depth-integrated rates of anammox in the Seine River sediments vary between 33 and 78 μmol cm^{-2} yr^{-1}, with higher values in the downstream than upstream sediments. The October pore water profiles also show measurable nitrite concentrations coexisting with high ammonium concentrations in the lower half of the cores, implying favorable chemical conditions for anammox at all depths except in the uppermost oxygenated sediment layers. The anammox rates estimated here are within the range reported for sediments in urban streams and wetlands (Shen et al., 2015; Wang et al., 2013; Table 1S).

4.4. Benthic exchange fluxes

The benthic exchange fluxes of nitrate, ammonium and nitrite are summarized in Fig. 6. As expected, the sediments act as sinks for nitrate. The benthic uptake fluxes of nitrate are higher at the downstream site,

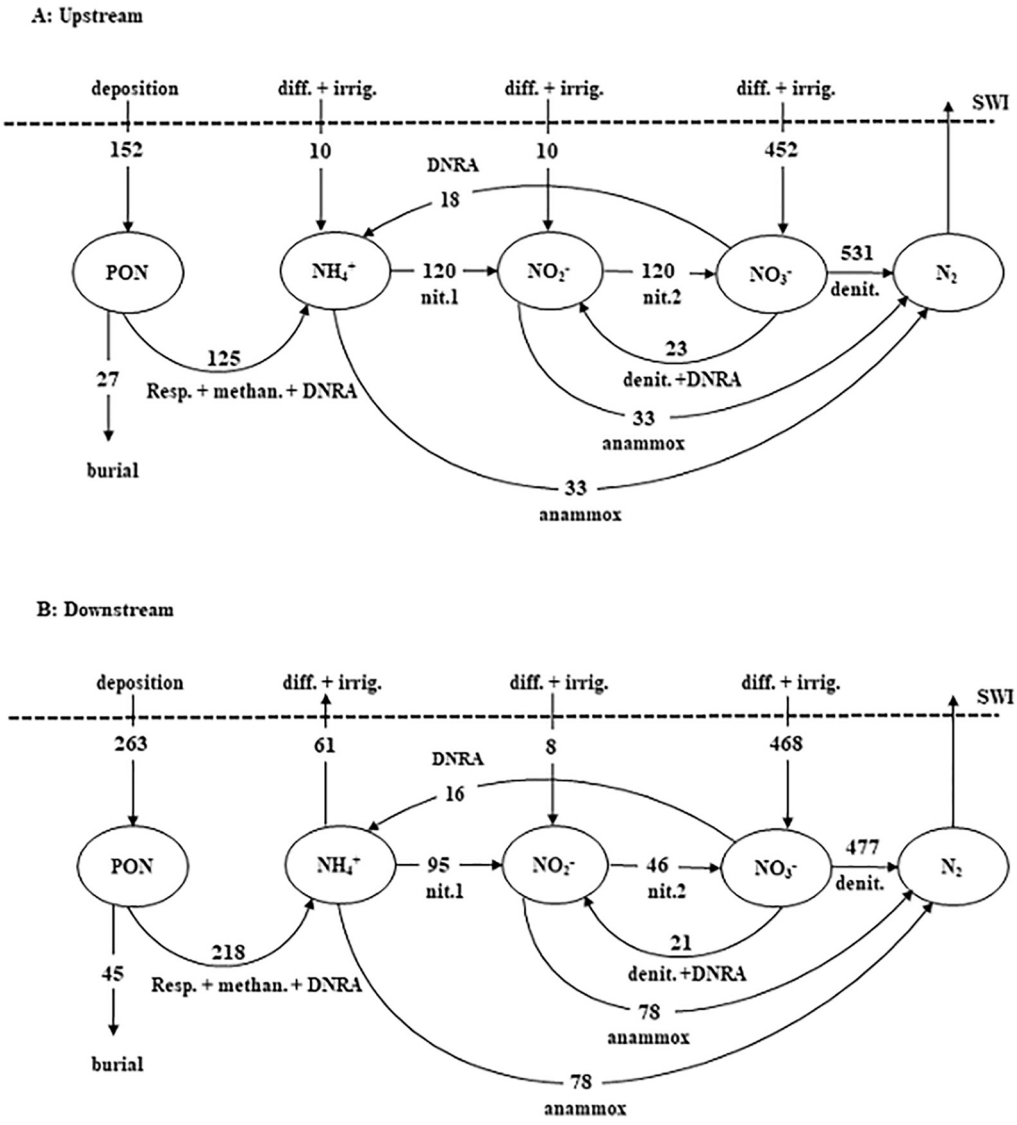

Fig. 4. Sediment nitrogen budgets. The values refer to model-derived, depth integrated reaction rates and fluxes (μmol cm^{-2} yr^{-1}) for the sites upstream (A) and downstream (B) of the SAV WWTP in August 2012. (diff.: diffusion; irrig.: irrigation; nit.1: nitrification step1; nit2.: nitrification setp2, methan.: methanogenesis; resp.: respiration).

and much higher in October than August. Both the core incubations and model results imply that the upstream sediments are a relatively small sink for ammonium, while the downstream sediments are a source of ammonium to the overlying water, due to the much larger production of ammonium from sediment organic matter degradation. A key difference in sediment N cycling between the sites is that the ammonium generated by organic matter breakdown is completely oxidized by nitrification and anammox within the sediment at the upstream site, while a large fraction is exported to the water column at the downstream site.

At both sites, sediments remove nitrite from the overlying water in August, but become nitrite sources to the overlying water in October. As with the other benthic N exchange fluxes, the magnitudes of the nitrite fluxes are higher in October than in August, and higher at the downstream site than the upstream site. There are few published benthic nitrite fluxes to which the fluxes obtained here can be compared. However, as can be seen from the literature values summarized in Table 7, existing studies report both influxes and effluxes of nitrite for a variety of freshwater and nearshore marine sediments, in agreement with the bidirectional nitrite fluxes observed for the Seine River sediments. Previous studies also highlight the roles of the bottom water O_2 (Höhener et al., 1994) and nitrate concentrations (Gardner and McCarthy, 2009), the C:N ratio of the organic matter in the topmost layer of sediment (Lerat, 1990), and the time of the year (Gardner and McCarthy, 2009; Kaiser et al., 2015), in controlling whether sediments are a source or sink of nitrite (Kaiser et al., 2015).

It is important to stress that the pore water N distributions (Figs. 2 and 3) and the benthic N fluxes (Fig. 6) represent data acquired independently from one another on separate sediment cores. The ability of the model to simultaneously account for the key features of the pore water profiles and the core incubation fluxes, as well as the general consistency of the model-predicted reaction rates and exchange fluxes with those reported for other freshwater depositional environments (Tables 6 and 1S), therefore supports the use of the model as a tool to predict nitrite benthic exchanges under variable environmental conditions. In particular, the directional switch of the nitrite fluxes can be attributed to the higher benthic oxygen demand in October compared to August, and the corresponding lower fractions of O_2 that are directed to nitrite oxidation (Table 5), hence resulting in excess nitrite production that is exported to the overlying water column.

The model also helps anticipate how benthic nitrite fluxes in the Seine River might respond to changes in WWTP discharges, bottom water chemistry or depositional fluxes. This is illustrated by the results of the sensitivity analyses in Fig. 7, which show that the O_2 concentration in the overlying water and the deposition flux of reactive organic matter exert key controls on the benthic nitrite fluxes. For the August conditions, setting the bottom water O_2 concentration to zero causes the sediments at both locations to switch from being sinks to becoming sources of nitrite to the overlying river water (see also Fig. 2S). For the October conditions, the sediments at both locations are a source of nitrite whether O_2 is present in the overlying water or not, but the

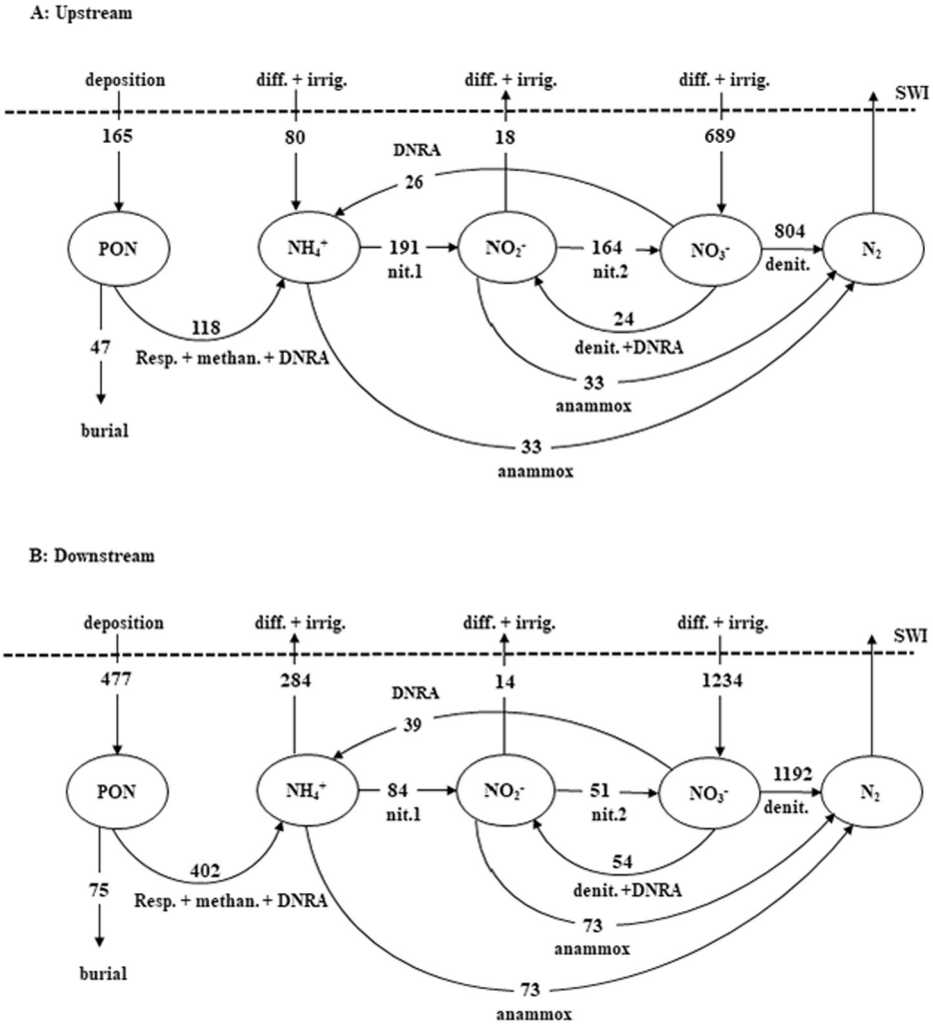

Fig. 5. Sediment nitrogen budgets. The values refer to model derived-depth, integrated reaction rates and fluxes (μmol cm^{-2} yr^{-1}) for the sites upstream (A) and downstream (B) of the SAV WWTP in October 2013. (diff.: diffusion; irrig.: irrigation; nit.1: nitrification step1; nit2.: nitrification setp2, methan.: methanogenesis; resp.: respiration).

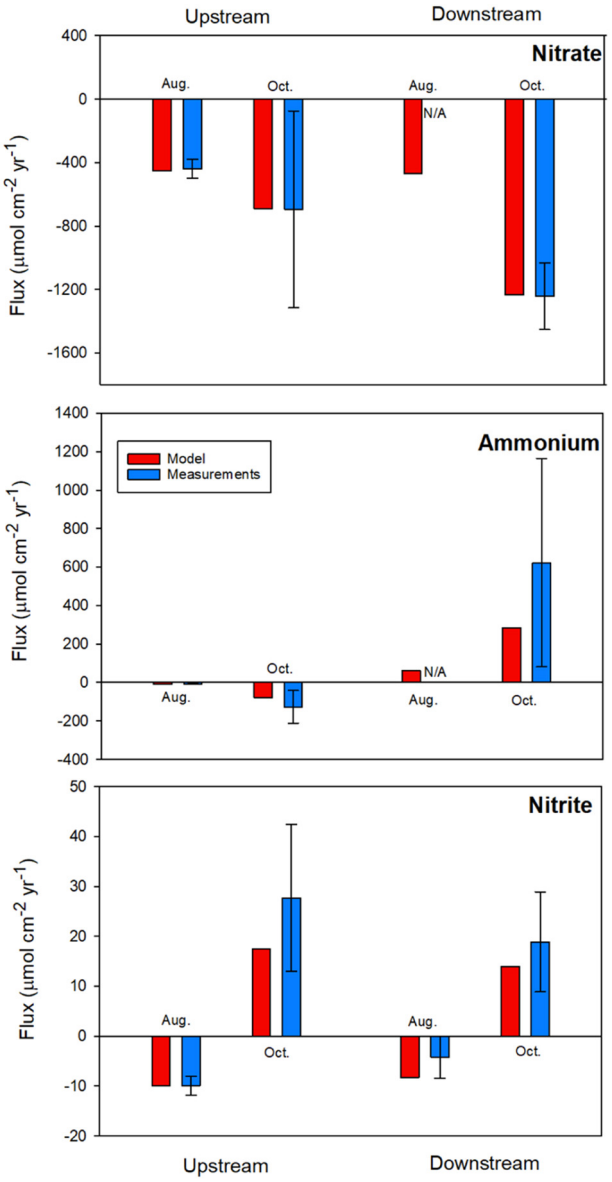

Fig. 6. Measured and modeled nitrate (A), ammonium (B) and nitrite fluxes (C) across the sediment water interface (SWI) at the sampling sites upstream and downstream of the SAV WWTP in August 2012 and October 2013. Error bars represent standard deviations on triplicate cores.

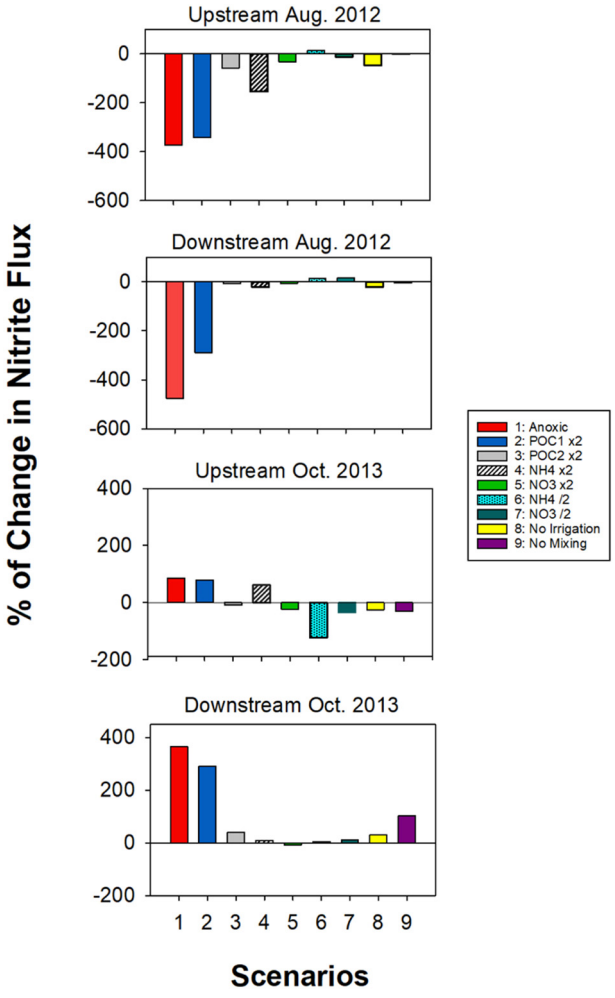

Fig. 7. Sensitivity analyses of the nitrite flux at the SWI based on different scenarios. Scenarios include no bottom water O_2 (Anoxic), doubled deposition flux of POC1 at the SWI (POC1 ×2), doubled deposition flux of POC2 at the SWI (POC2 ×2), doubled concentrations of ammonium and nitrate in the overlying water (NH_4 ×2, NO_3 ×2, respectively), and halving concentrations of ammonium and nitrate in the overlying water (NH_4 /2, NO_3 /2, respectively). No irrigation corresponds to a simulation where a zero value was imposed to the pore water irrigation coefficient (α) and no mixing represents a simulation where a zero value was imposed to the sediment mixing coefficient (D_B). Negative changes imply a change in the direction of the benthic nitrite flux.

magnitude of the benthic efflux is much higher in the absence of O_2. The large increase in nitrite efflux under O_2 depleted bottom waters is due to the cessation of nitrification, which no longer prevents pore water nitrite from escaping to the overlying water column.

The deposition flux of reactive organic carbon (POC1) significantly impacts benthic nitrite exchanges (Figs. 7 and 8), because it directly affects the production of pore water nitrite by denitrification. As shown in Fig. 8, the nitrite benthic flux correlates positively with the supply of POC1 to the sediments, although the trends differ between the two locations and between the two sampling times. The POC1 deposition flux at

Table 7
Benthic nitrite fluxes reported in the literature; positive values indicate efflux to the water column, negative values indicate sediment uptake fluxes.

Location	Benthic nitrite fluxes at the SWI (μmol N cm^{-2} yr^{-1})	Explanation	References
Lake Sempach, Switzerland	+3.6 to +14.7	Deep, eutrophic and artificially oxygenated	(Höhener et al., 1994)
Lake Taihu, China	−27.1	Shallow and eutrophic	(McCarthy et al., 2007)
Guarapiranga reservoir, Brazil	+100.0	Eutrophic, located in a highly populated and industrialized area	(Mozeto et al., 2001)
Mangrove sediments, China	−15.0 to +32.4	Under light and dark condition in two seasons	(Kaiser et al., 2015)
Morlaix Bay, France	−9.5 to +8.1	Seasonal variations during a year	(Lerat, 1990)
Florida Bay, US	−1.5 to +1.9	Shallow subtropical	(Gardner and McCarthy, 2009)
Florida Bay, US	−1.3 to +45.5	After addition of nitrate in the overlying water	(Gardner and McCarthy, 2009)
Seine River, France	−8.3 to +17.5	Upstream and downstream of the SAV WWTP	(Modeled, this study)

which the sediments switch from sink to source of nitrite is two to three times lower under the October than August conditions, in part because of the more vigorous pore water irrigation in October compared to August (Tables 4a and 4b), which promotes the export of nitrite to the overlying water. Under the October conditions, the POC1 deposition flux at the two sites would have to drop below 1000 μmol cm^{-2} yr^{-1} in order for the sediments to become nitrite sinks. Not surprisingly, the deposition flux of the less reactive POC2 has much less of an effect on the benthic nitrite fluxes than POC1.

Bottom water ammonium concentrations affect the benthic nitrite fluxes by impacting nitrification (nitrite source) and anammox (nitrite sink). Sensitivity to changes in bottom water ammonium is relatively higher at the upstream site, because of the important role of nitrification in producing pore water nitrite (Figs. 4 and 5). In the downstream sediments, where anammox is a major sink of nitrite, the effects of changes in bottom water ammonium on nitrification and anammox tend to balance each other out. In a similar vein, changes in bottom water nitrate concentrations result in opposing effects of denitrification (nitrite source) and anammox (nitrite sink). Hence, the benthic nitrite fluxes tend to be relatively insensitive to changing bottom water nitrate concentrations.

4.5. Nitrite budget

The experimental and modeling results show that the Seine sediments at the two locations can act as either a source or sink of nitrite. This raises the question of the role of benthic exchanges on the nitrite budget of the river. A full assessment of this role would require the systematic (seasonal) acquisition of benthic nitrite exchange data along the entire course of the river. Here, we provide rough estimations of the potential benthic nitrite supply and removal using a maximum nitrite efflux of around 30 μmol cm^{-2} yr^{-1}, as measured in October 2013 at the downstream site, and a maximum influx of around 10 μmol cm^{-2} yr^{-1}, as measured in the August incubations (Fig. 6). Over a 300 km-long stretch of the Seine River, and for a representative width of 200 m plus an assumed 10% coverage by nitrite-exchanging streambed sediments, this results in an annual maximum benthic nitrite release of 6×10^5 mol yr^{-1} and a maximum uptake of 2×10^5 mol yr^{-1}. In comparison, the SAV WWTP discharged on average 6×10^7 mol yr^{-1} of nitrite between 2007 and 2013 (Aissa-Grouz et al., 2015), that is two orders of magnitude higher than the calculated benthic exchanges. Although our preliminary calculations need further corroboration, at this stage it appears that the benthic exchanges are a relatively small component of the Seine River nitrite budget downstream of the WWTP. If this is true, then the persistence of measurable nitrite concentrations as far as 300 km downstream of Paris despite fully aerated conditions (Aissa-Grouz et al., 2015) may be due to the combination of high nitrite release from the SAV WWTP, high river discharge and low nitrification activity in the water column (Raimonet et al., 2017).

5. Concluding remarks

With the model presented in this paper we have analyzed how benthic nitrite exchanges in the Seine River are modulated by environmental conditions at, and early diagenetic processes below, the SWI. The model accounts for the key features of the observed pore water profiles of the different nitrogen species while at the same time reproducing the measured benthic fluxes of nitrate, nitrite and ammonium; it captures the differences between the sediments collected upstream and downstream of the SAV WWTP, and between the summer and fall sampling times. While the modeling results imply that denitrification dominates N cycling in the sediments, they also highlight the important roles of other transformation pathways, especially nitrification and anammox, and (bio)physical mixing processes in determining the distributions and benthic fluxes of the various N species. In particular, the model explains why, depending on the site location and sampling time, the sediments either release nitrite to the overlying water column or remove it. The simulation results further indicate that the SAV WWTP not only impacts downstream benthic nitrite fluxes through the discharge of N species contained in its effluents, but also by affecting the supply of labile organic matter and the dissolved oxygen concentration at the sediment-water interface.

As illustrated here for a comprehensive data set on N species, early diagenetic modeling can be a powerful tool for analyzing benthic transformations and fluxes in highly dynamic systems such as streambed sediments. Mechanistic modeling forces us to question our understanding of the processes and their interactions within sediments that give rise to the observed pore water geochemistry and benthic exchanges. As such, the modeling provides complementary information that cannot be deduced directly from the data alone. With the rapid improvement of

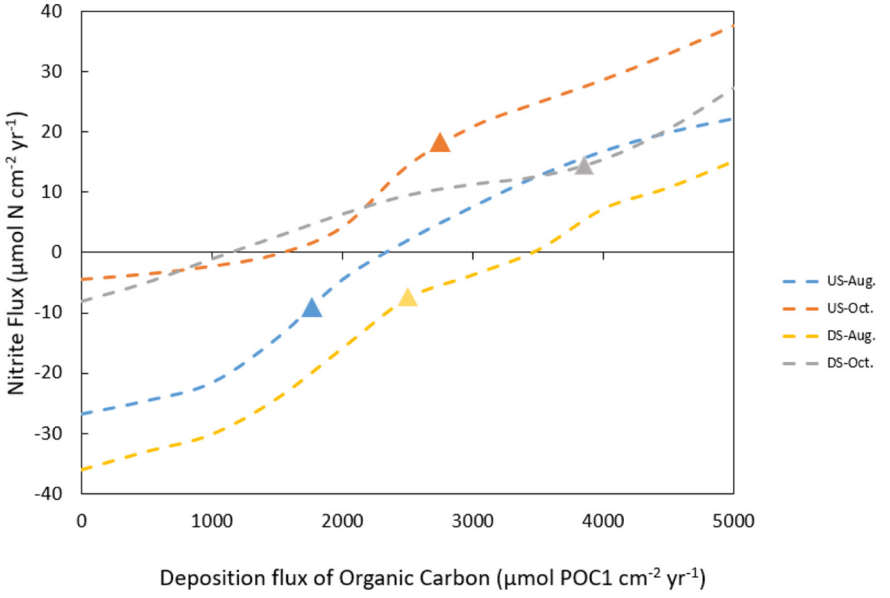

Fig. 8. Nitrite fluxes across the SWI as a function of deposition flux of the most reactive organic carbon, POC1. Symbols correspond to fluxes simulated with the model-calibrated POC1 deposition fluxes at the two sites (US = upstream, DS = downstream) and two sampling times (August and October). Positive fluxes indicate nitrite efflux from sediment to water column, negative fluxes indicate uptake of nitrite by the sediments.

analytical capabilities, including in situ microsensors, it is becoming increasingly routine to measure the relatively low concentrations of reactive intermediates in biogeochemical reaction networks. This creates an increasing demand for environmental reactive transport models that explicitly simulate the production, consumption and transport of reactive intermediates, as done here for nitrite. The model developed in this study should be broadly applicable to sediments in freshwater aquatic environments receiving high N and organic matter loads.

Acknowledgements

Funding for this project was provided by the Canada Excellence Research Chair (CERC) program, a Strategic Partnership Grant (STPGP447692-2013, PI Sherry Schiff) from the Natural Sciences and Engineering Research Council of Canada (NSERC), and the PIREN SEINE and R2DS Île de France programs. ZA also acknowledges the financial support from TERRE-CREATE, funded through NSERC's Collaborative Research and Training Experience (CREATE) Program, to attend reactive transport modeling courses at the University of Waterloo and University of British Columbia. We also thank Vincent Rocher, Julien Pouillaude and Erwan Garcia-Gonzalez of SIAAP (Syndicat Interdépartemental pour l'Assainissement de l'Agglomération Parisienne) for logistical help with sampling the Seine River sediment cores. The authors are grateful to Dr. Sherry Schiff, Dr. Nandita Basu and Dr. Hans Dürr for constructive discussions. Comments of the two journal reviewers helped strengthen the manuscript.

Appendix A. Supplementary data

Supplementary data to this article can be found online at https://doi.org/10.1016/j.scitotenv.2018.01.319.

References

Aissa-Grouz, N., Garnier, J., Billen, G., Mercier, B., Martinez, A., 2015. The response of river nitrification to changes in wastewater treatment (the case of the lower Seine River downstream from Paris). Ann. Limnol. Int. J. Limnol. 51:351–364. https://doi.org/10.1051/limn/2015031.

Altmann, D., Stief, P., Amann, R., De Beer, D., Schramm, A., 2003. Brief report in situ distribution and activity of nitrifying bacteria in freshwater sediment. Environ. Microbiol. 5:798–803. https://doi.org/10.1046/j.1462-2920.2003.00469.x.

Babbin, A.R., Ward, B.B., 2013. Controls on nitrogen loss processes in Chesapeake Bay sediments. Environ. Sci. Technol. 47 (9):4189–4196. https://doi.org/10.1021/es304842r.

Beaulieu, J.J., Arango, C.P., Hamilton, S.K., Tank, J.L., 2007. The production and emission of nitrous oxide from headwater streams in the Midwestern United States. Glob. Chang. Biol. 14:878–894. https://doi.org/10.1111/j.1365-2486.2007.01485.x.

Billen, G., Garnier, J., Némery, J., Sebilo, M., Sferratore, A., Barles, S., Benoit, P., Benoît, M., 2007. A long-term view of nutrient transfers through the Seine River continuum. Sci. Total Environ. 375:80–97. https://doi.org/10.1016/j.scitotenv.2006.12.005.

Boudreau, B.P., 1996. A method-of-lines code for carbon and nutrient diagenesis in aquatic sediments. Comput. Geosci. 22, 479–496.

Boudreau, B.P., 1997. Diagenetic Models and Their Implementation. Springer, Berlin, Germany.

Canavan, R.W., Slomp, C.P., Jourabchi, P., Van Cappellen, P., Laverman, A.M., van den Berg, G.A., 2006. Organic matter mineralization in sediment of a coastal freshwater lake and response to salinization. Geochim. Cosmochim. Acta 70:2836–2855. https://doi.org/10.1016/j.gca.2006.03.012.

Canavan, R.W., Laverman, A.M., Slomp, C.P., 2007. Modeling nitrogen cycling in a coastal fresh water sediment. Hydrobiologia 584:27–36. https://doi.org/10.1007/s10750-007-0583-z.

Cébron, A., Garnier, J., 2005. Nitrobacter and Nitrospira genera as representatives of nitrite-oxidizing bacteria: detection, quantification and growth along the lower Seine River (France). Water Res. 39:4979–4992. https://doi.org/10.1016/j.watres.2005.10.006.

Chesterikoff, A., Garban, B., Billen, G., Poulin, M., 1992. Inorganic nitrogen dynamics in the river seine downstream from Paris (France). Biogeochemistry 17, 147–164.

Clevinger, C.C., Heath, R.T., Bade, D.L., 2014. Oxygen use by nitrification in the hypolimnion and sediments of Lake Erie. J. Great Lakes Res. 40:202–207. https://doi.org/10.1016/j.jglr.2013.09.015.

Clough, T.J., Bertram, J.E., Sherlock, R.R., Leonard, R.L., Nowicki, B.L., 2006. Comparison of measured and EF5-r-derived N_2O fluxes from a spring-fed river. Glob. Chang. Biol. 12:352–363. https://doi.org/10.1111/j.1365-2486.2005.01089.x.

Cooper, A.B., 1984. Activities of benthic nitrifiers in streams and their role in oxygen consumption. Microb. Ecol. 10:317–334. https://doi.org/10.1007/BF02015557.

Couture, R.-M., Shafei, B., Van Cappellen, P., Tessier, A., Gobeil, C., 2010. Non-steady state modeling of arsenic diagenesis in lake sediments. Environ. Sci. Technol. 44:197–203. https://doi.org/10.1021/es902077q.

Cowling, E.B., Erisman, J.W., Smeulders, S.M., Holman, S.C., Nicholson, B.M., 1998. Optimizing air quality management in Europe and North America: justification for integrated management of both oxidized and reduced forms of nitrogen. Environ. Pollut. 102:599–608. https://doi.org/10.1016/S0269-7491(98)80088-2.

Crowe, S.A., Treusch, A.H., Forth, M., Li, J., Magen, C., Canfield, D.E., Thamdrup, B., Katsev, S., 2017. Novel anammox bacteria and nitrogen loss from Lake Superior. Sci. Rep. 7: 1–7. https://doi.org/10.1038/s41598-017-12270-1.

Crutzen, P.J., Mosier, A.R., Smith, K.A., Winiwarter, W., 2007. N_2O release from agro-biofuel production negates global warming reduction by replacing fossil fuels. Atmos. Chem. Phys. Discuss. 7:11191–11205. https://doi.org/10.5194/acpd-7-11191-2007.

Dale, A.W., Regnier, P., Knab, N.J., Jørgensen, B.B., Van Cappellen, P., 2008. Anaerobic oxidation of methane (AOM) in marine sediments from the Skagerrak (Denmark): II. Reaction-transport modeling. Geochim. Cosmochim. Acta 72:2880–2894. https://doi.org/10.1016/j.gca.2007.11.039.

Dale, a.W., Sommer, S., Bohlen, L., Treude, T., Bertics, V.J., Bange, H.W., Pfannkuche, O., Schorp, T., Mattsdotter, M., Wallmann, K., 2011. Rates and regulation of nitrogen cycling in seasonally hypoxic sediments during winter (Boknis Eck, SW Baltic Sea): sensitivity to environmental variables. Estuar. Coast. Shelf Sci. 95:14–28. https://doi.org/10.1016/j.ecss.2011.05.016.

Devallois, V., Boyer, P., Boudenne, J.L., Coulomb, B., 2008. Modelling the vertical profiles of O_2 and pH in saturated freshwater sediments. Ann. Limnol. Int. J. Limnol. 44:275–288. https://doi.org/10.1051/limn:2008011.

Diaz, R.J., Rosenberg, R., 2008. Spreading dead zones and consequences for marine ecosystems. Science 321:926–929 (80-.). https://doi.org/10.1126/science.1156401.

Driscoll, C., Whitall, D., Aber, J., Boyer, E., Castro, M., Cronan, C., Goodale, C.L., Groffman, P., Hopkinson, C., Lambert, K., Lawrence, G., Ollinger, S., 2003. Nitrogen pollution in the Northeastern United States: sources, effects, and management options. Bioscience 53.

Erisman, J.W., Galloway, J.N., Seitzinger, S., Bleeker, A., Dise, N.B., Petrescu, A.M.R., Leach, A.M., de Vries, W., 2013. Consequences of human modification of the global nitrogen cycle. Philos. Trans. R. Soc. B Biol. Sci. 368:20130116. https://doi.org/10.1098/rstb.2013.0116.

Garban, B., Ollivon, D., Poulin, M., Gaultier, V., Chesterikoff, A., 1995. Exchanges at the sediment-water interface in the river seine, downstream from Paris. Water Res. 29: 473–481. https://doi.org/10.1016/0043-1354(94)00181-6.

García-Ruiz, R., Pattinson, S.N., Whitton, B.A., 1998. Kinetic parameters of denitrification in a river continuum. Appl. Environ. Microbiol. 64, 2533–2538.

Gardner, W.S., McCarthy, M.J., 2009. Nitrogen dynamics at the sediment–water interface in shallow, sub-tropical Florida Bay: why denitrification efficiency may decrease with increased eutrophication. Biogeochemistry 95:185–198. https://doi.org/10.1007/s10533-009-9329-5.

Gardner, W.S., Mccarthy, M.J., An, S., Sobolev, D., Sell, K.S., Brock, D., 2006. Nitrogen Fixation and Dissimilatory Nitrate Reduction to Ammonium (DNRA) Support Nitrogen Dynamics in Texas Estuaries. 51 pp. 558–568.

Garnier, J., Cébron, A., Tallec, G., Billen, G., Sebilo, M., Martinez, A., 2006. Nitrogen behaviour and nitrous oxide emission in the tidal Seine River estuary (France) as influenced by human activities in the upstream watershed. Biogeochemistry 77:305–326. https://doi.org/10.1007/s10533-005-0544-4.

Gruber, N., Galloway, J.N., 2008. An earth-system perspective of the global nitrogen cycle. Nature 451:293–296. https://doi.org/10.1038/nature06592.

Hall, G.H., Jeffries, C., 1984. The contribution of nitrification in the water column and profundal sediments to the total oxygen deficit of the hypolimnion of a mesotrophic lake (Grasmere, English Lake District). Microb. Ecol. 10:37–46. https://doi.org/10.1007/BF02011593.

Han, H., Lu, X., Burger, D.F., Joshi, U.M., Zhang, L., 2014. Nitrogen dynamics at the sediment–water interface in a tropical reservoir. Ecol. Eng. 73:146–153. https://doi.org/10.1016/j.ecoleng.2014.09.016.

Höhener, P., Gächter, R., Sciences, A., Science, E., Re-, L., 1994. Nitrogen cycling across the sediment-water interface in an eutrophic, artificially oxygenated lake. Aquat. Sci. 56: 115–132. https://doi.org/10.1007/BF00877203.

Kaiser, D., Kowalski, N., Böttcher, M., Yan, B., Unger, D., 2015. Benthic nutrient fluxes from mangrove sediments of an anthropogenically impacted estuary in Southern China. J. Mar. Sci. Eng. 3:466–491. https://doi.org/10.3390/jmse3020466.

Keffala, C., Galleguillos, M., Ghrabi, A., Vasel, J.L., 2011. Investigation of nitrification and denitrification in the sediment of wastewater stabilization ponds. Water Air Soil Pollut. 219:389–399. https://doi.org/10.1007/s11270-010-0715-3.

Kelso, B.H.L., Smith, R.V., Laughlin, R.J., Lennox, S.D., 1997. Dissimilatory nitrate reduction in anaerobic sediments leading to river nitrite accumulation. Appl. Environ. Microbiol. 63, 4679–4685.

Knobeloch, L., Salna, B., Hogan, A., Postle, J., Anderson, H., 2000. Blue babies and nitrate-contaminated well water. Environ. Health Perspect. 108:675–678. https://doi.org/10.1289/ehp.00108675.

Krumins, V., Gehlen, M., Arndt, S., Van Cappellen, P., Regnier, P., 2013. Dissolved inorganic carbon and alkalinity fluxes from coastal marine sediments: model estimates for different shelf environments and sensitivity to global change. Biogeosciences 10: 371–398. https://doi.org/10.5194/bg-10-371-2013.

Laursen, A.E., Seitzinger, S.P., 2002. Measurement of denitrification in rivers: an integrated, whole reach approach. Hydrobiologia 485:67–81. https://doi.org/10.1023/A:1021398431995.

Laverman, A.M., Meile, C., Van Cappellen, P., Wieringa, E.B.A., 2007. Vertical distribution of denitrification in an estuarine sediment: integrating sediment flowthrough reactor experiments and microprofiling via reactive transport modeling. Appl. Environ. Microbiol. 73:40–47. https://doi.org/10.1128/AEM.01442-06.

Laverman, A.M., Garnier, J.A., Mounier, E.M., Roose-Amsaleg, C.L., 2010. Nitrous oxide production kinetics during nitrate reduction in river sediments. Water Res. 44: 1753–1764. https://doi.org/10.1016/j.watres.2009.11.050.
Lecroart, P., Schmidt, S., Anschutz, P., Jouanneau, J.-M., 2007. Modeling sensitivity of biodiffusion coefficient to seasonal bioturbation. J. Mar. Res. 65:417–440. https://doi.org/10.1357/002224007781567630.
Lerat, Y., 1990. Seasonal changes in pore water concentrations of nutrients and their diffusive fluxes at the sediment-water. J. Exp. Mar. Biol. Ecol. 135:135–160. https://doi.org/10.1016/0022-0981(90)90012-2.
Massoudieh, A., Bombardelli, F.A., Ginn, T.R., 2010. A biogeochemical model of contaminant fate and transport in river waters and sediments. J. Contam. Hydrol. 112: 103–117. https://doi.org/10.1016/j.jconhyd.2009.11.001.
McCarthy, M.J., Lavrentyev, P.J., Yang, L., Zhang, L., Chen, Y., Qin, B., Gardner, W.S., 2007. Nitrogen dynamics and microbial food web structure during a summer cyanobacterial bloom in a subtropical, shallow, well-mixed, eutrophic lake (Lake Taihu, China). Hydrobiologia 581:195–207. https://doi.org/10.1007/s10750-006-0496-2.
Meile, C., Van Cappellen, P., 2003. Global estimates of enhanced solute transport in marine sediments. Limnol. Oceanogr. 48:777–786. https://doi.org/10.4319/lo.2003.48.2.0777.
Meyer, R.L., Risgaard-Petersen, N., Allen, D.E., 2005. Correlation between anammox activity and microscale distribution of nitrite in a subtropical mangrove sediment. Appl. Environ. Microbiol. 71:6142–6149. https://doi.org/10.1128/AEM.71.10.6142-6149.2005.
Meyer, R.L., Allen, D.E., Schmidt, S., 2008. Nitrification and denitrification as sources of sediment nitrous oxide production: a microsensor approach. Mar. Chem. 110: 68–76. https://doi.org/10.1016/j.marchem.2008.02.004.
Mordy, C.W., Eisner, L.B., Proctor, P., Stabeno, P., Devol, A.H., Shull, D.H., Napp, J.M., Whitledge, T., 2010. Temporary uncoupling of the marine nitrogen cycle: accumulation of nitrite on the Bering Sea shelf. Mar. Chem. 121:157–166. https://doi.org/10.1016/j.marchem.2010.04.004.
Mozeto, A.A., Silvério, P.F., Soares, A., 2001. Estimates of benthic fluxes of nutrients across the sediment-water interface (Guarapiranga reservoir, Sao Paulo, Brazil). Sci. Total Environ. 266:135–142. https://doi.org/10.1016/S0048-9697(00)00726-9.
Naeher, S., Huguet, A., Roose-Amsaleg, C.L., Laverman, A.M., Fosse, C., Lehmann, M.F., Derenne, S., Zopfi, J., 2015. Molecular and geochemical constraints on anaerobic ammonium oxidation (anammox) in a riparian zone of the Seine Estuary (France). Biogeochemistry https://doi.org/10.1007/s10533-014-0066-z.
Ndegwa, P.M., Hristov, A.N., Arogo, J., Sheffield, R.E., 2008. A review of ammonia emission mitigation techniques for concentrated animal feeding operations. Biosyst. Eng. 100: 453–469. https://doi.org/10.1016/j.biosystemseng.2008.05.010.
Oenema, O., Bleeker, A., Braathen, N.A., Budňáková, M., Bull, K., Čermák, P., Geupel, M., Hicks, K., Hoft, R., Kozlova, N., Leip, A., Spranger, T., Valli, L., Velthof, G., Winiwarter, W., 2011. Nitrogen in current European policies. Eur. Nitrogen Assess. 62–81.
Paraska, D.W., Hipsey, M.R., Salmon, S.U., 2014. Sediment diagenesis models: review of approaches, challenges and opportunities. Environ. Model. Softw. 61:297–325. https://doi.org/10.1016/j.envsoft.2014.05.011.
Pauer, J., 2000. Nitrification in the water column and sediment of a hypereutrophic lake and adjoining river system. Water Res. 34:1247–1254. https://doi.org/10.1016/S0043-1354(99)00258-4.
Philips, S., Laanbroek, H.J., Verstraete, W., 2002. Origin, causes and effects of increased nitrite concentrations in aquatic environments. Rev. Environ. Sci. Bio/Technology 1: 115–141. https://doi.org/10.1023/A:1020892826575.
Rabalais, N.N., Díaz, R.J., Levin, L.A., Turner, R.E., Gilbert, D., Zhang, J., 2010. Dynamics and distribution of natural and human-caused hypoxia. Biogeosciences 7:585–619. https://doi.org/10.5194/bg-7-585-2010.
Raimonet, M., Vilmin, L., Flipo, N., Rocher, V., Laverman, A.M., 2015. Modelling the fate of nitrite in an urbanized river using experimentally obtained nitrifier growth parameters. Water Res. 73:373–387. https://doi.org/10.1016/j.watres.2015.01.026.
Raimonet, M., Cazier, T., Rocher, V., Laverman, A.M., 2017. Nitrifying kinetics and the persistence of nitrite in the Seine River, France. J. Environ. Qual. 595:585–595. https://doi.org/10.2134/jeq2016.06.0242.
Revsbech, N.P., 1989. An oxygen microsensor with a guard cathode. Limnol. Oceanogr. 34: 474–478. https://doi.org/10.4319/lo.1989.34.2.0474.
Revsbech, N.P., Jørgensen, B.B., 1986. Microelectrodes: their use in microbial ecology. In: Marshall, K.C. (Ed.), Advances in Microbial Ecology. Springer US, pp. 293–352.
Richardson, D., Felgate, H., Watmough, N., Thomson, A., Baggs, E., 2009. Mitigating release of the potent greenhouse gas N_2O from the nitrogen cycle – could enzymic regulation hold the key? Trends Biotechnol. 27:388–397. https://doi.org/10.1016/j.tibtech.2009.03.009.
Rocher, V., Garcia-Gonzalez, E., Paffoni, C., Thomas, W., 2015. La production de nitrites lors de la dénitrification des eaux usées : un sujet sensible et complexe!L'Eau, l'Industrie, les Nuisances 344. pp. 80–83.
Rodier, J., 1984. In: Dunod (Ed.), L'analyse de l'eau (eaux naturelles, eaux re´ siduaires, eau de mer), Seventh ed, Paris (1364 pp.).
Rong, N., Shan, B., Wang, C., 2016. Determination of sediment oxygen demand in the Ziya River Watershed, China: based on laboratory core incubation and microelectrode measurements. Int. J. Environ. Res. Public Health 13:232. https://doi.org/10.3390/ijerph13020232.
Rosamond, M.S., Thuss, S.J., Schiff, S.L., 2012. Dependence of riverine nitrous oxide emissions on dissolved oxygen levels. Nat. Geosci. 5:715–718. https://doi.org/10.1038/ngeo1556.
Rysgaard, S., Risgaard-Petersen, N., Sloth, N.P., Jensen, K., Nielsen, L.P., 1994. Oxygen regulation of nitrification and denitrification in freshwater sediments. Limnol. Oceanogr. 39, 1643–1652.
Seitzinger, S.P., 1988. Denitrification in freshwater and coastal marine ecosystems: ecological and geochemical significance. Limnol. Oceanogr. 33:702–724. https://doi.org/10.4319/lo.1988.33.4_part_2.0702.
Shen, L., Liu, S., He, Z., Lian, X., Huang, Q., He, Y., Lou, L., Xu, X., Zheng, P., Hu, B., 2015. Depth-specific distribution and importance of nitrite-dependent anaerobic ammonium and methane-oxidising bacteria in an urban wetland. Soil Biol. Biochem. 83: 43–51. https://doi.org/10.1016/j.soilbio.2015.01.010.
Stein, L.Y., 2015. Microbiology: cyanate fuels the nitrogen cycle. Nature 524:43–44. https://doi.org/10.1038/nature14639.
Stief, P., de Beer, D., 2006. Probing the microenvironment of freshwater sediment macrofauna: implications of deposit-feeding and bioirrigation for nitrogen cycling. Limnol. Oceanogr. 51:2538–2548. https://doi.org/10.4319/lo.2006.51.6.2538.
Stief, P., Beer, D., Neumann, D., 2002. Small-scale distribution of interstitial nitrite in freshwater sediment microcosms: the role of nitrate and oxygen availability, and sediment permeability. Microb. Ecol. 43:367–377. https://doi.org/10.1007/s00248-002-2008-x.
Strauss, E.A., Richardson, W.B., Bartsch, L.A., Cavanaugh, J.C., Bruesewitz, D.A., Imker, H., Heinz, J.A., Soballe, D.M., 2004. Nitrification in the Upper Mississippi River: patterns, controls , and contribution to the NO_3- budget. J. North Am. Benthol. Soc. 23:1–14. https://doi.org/10.1899/0887-3593(2004)023<0001:NITUMR>2.0.CO;2.
Strous, M., Kuenen, J.G., Jetten, M.S.M., 1999. Key physiology of anaerobic ammonium oxidation. Appl. Environ. Microbiol. 65, 3248–3250.
Sweerts, J.-P.R.A., de Beer, D., 1989. Microelectrode measurements of nitrate gradients in the littoral and profundal sediments of a meso-eutrophic Lake (Lake Vechten, The Netherlands). Appl. Environ. Microbiol. 55, 754–757.
Thamdrup, B.O., Dalsgaard, T., 2008. Nitrogen cycling in sediments. In: Kirchman, D.L. (Ed.), Microbial Ecology of the Oceans, 2nd edition John Wiley & Sons Inc., Hoboken, New Jersey, pp. 527–568.
Thouvenot, M., Billen, G., Garnier, J., 2007. Modelling nutrient exchange at the sediment–water interface of river systems. J. Hydrol. 341:55–78. https://doi.org/10.1016/j.jhydrol.2007.05.001.
Thouvenot-Korppoo, M., Billen, G., Garnier, J., 2009. Modelling benthic denitrification processes over a whole drainage network. J. Hydrol. 379:239–250. https://doi.org/10.1016/j.jhydrol.2009.10.005.
Tomaszek, J.A., Czerwieniec, E., 2000. In situ chamber denitrification measurements in reservoir sediments: an example from southeast Poland. Ecol. Eng. 16:61–71. https://doi.org/10.1016/S0925-8574(00)00090-2.
Tomaszek, J.A., Czerwieniec, E., 2003. Dentrification and oxygen consumption in bottom sediments: factors influencing rates of the processes. Hydrobiologia 504:59–65. https://doi.org/10.1023/B:HYDR.0000008508.81690.10.
Torres, E., Couture, R.M., Shafei, B., Nardi, A., Ayora, C., Van Cappellen, P., 2015. Reactive transport modeling of early diagenesis in a reservoir lake affected by acid mine drainage: trace metals, lake overturn, benthic fluxes and remediation. Chem. Geol. 419: 75–91. https://doi.org/10.1016/j.chemgeo.2015.10.023.
Trimmer, M., Nicholls, J.C., Morley, N., Davies, C.A., Aldridge, J., 2005. Biphasic behavior of anammox regulated by nitrite and nitrate in an estuarine sediment biphasic behavior of anammox regulated by nitrite and nitrate in an estuarine sediment. Society 71: 1923–1930. https://doi.org/10.1128/AEM.71.4.1923.
Trinh, A.D., Meysman, F., Rochelle-Newall, E., Bonnet, M.P., 2012. Quantification of sediment-water interactions in a polluted tropical river through biogeochemical modeling. Glob. Biogeochem. Cycles 26:1–15. https://doi.org/10.1029/2010GB003963.
Udert, K.M., Larsen, T.A., Gujer, W., 2005. Chemical nitrite oxidation in acid solutions as a consequence of microbial ammonium oxidation. Environ. Sci. Technol. 39: 4066–4075. https://doi.org/10.1021/es048422m.
Van Cappellen, P., Wang, Y., 1995. Metal cycling in sediments: modeling the interplay of reaction and transport. In: Allen, H.E. (Ed.), Metal Contaminated Aquatic Sediments. Ann Arbor Press, Chelsea, pp. 21–64.
Van Den Berg, G.A., Gustav Loch, J.P., Van Der Heijdt, L.M., Zwolsman, J.J.G., 2000. Redox processes in recent sediments of the river Meuse, The Netherlands. Biogeochemistry 48:217–235. https://doi.org/10.1023/A:1006268325889.
Vilmin, L., Escoffier, N., Groleau, A., Poulin, M., Flipo, N., 2014. Modelling Algae Growth and Dissolved Oxygen in the Seine River Downstream the Paris Urban Area: Contribution of High Frequency Measurements. 16 p. 7748.
Vilmin, L., Aissa-Grouz, N., Garnier, J., Billen, G., Mouchel, J.-M., Poulin, M., Flipo, N., 2015. Impact of hydro-sedimentary processes on the dynamics of soluble reactive phosphorus in the Seine River. Biogeochemistry 122:229–251. https://doi.org/10.1007/s10533-014-0038-3.
Wang, Y., Van Cappellen, P., 1996. A multicomponent reactive transport model of early diagenesis: application to redox cycling in coastal marine sediments. Geochim. Cosmochim. Acta 60:2993–3014. https://doi.org/10.1016/0016-7037(96)00140-8.
Wang, Y., Li, Z., Zhou, L., Feng, L., Fan, N., Shen, J., 2013. Effects of macrophyte-associated nitrogen cycling bacteria on denitrification in the sediments of the eutrophic Gonghu Bay, Taihu Lake. Hydrobiologia 700:329–341. https://doi.org/10.1007/s10750-012-1241-7.
Ward, B.B., 2013. Nitrification. Reference Module in Earth Systems and Environmental Sciences. Elsevier:pp. 1–8 https://doi.org/10.1016/B978-0-12-409548-9.00697-7.
von der Wiesche, M., Wetzel, A., 1998. Temporal and spatial dynamics of nitrite accumulation in the River Lahn. Water Res. 32:1653–1661. https://doi.org/10.1016/S0043-1354(97)00376-X.
Yoshinaga, I., Amano, T., Yamagishi, T., Okada, K., Ueda, S., Sako, Y., Suwa, Y., 2011. Distribution and diversity of anaerobic ammonium oxidation (anammox) bacteria in the sediment of a eutrophic freshwater Lake, Lake Kitaura, Japan. Microbes Environ. 26: 189–197. https://doi.org/10.1264/jsme2.ME10184.
Zhao, Y., Xia, Y., Kana, T.M., Wu, Y., Li, X., Yan, X., 2013. Seasonal variation and controlling factors of anaerobic ammonium oxidation in freshwater river sediments in the Taihu Lake region of China. Chemosphere 93:2124–2131. https://doi.org/10.1016/j.chemosphere.2013.07.063.
Zhu, G., Wang, S., Wang, W., Wang, Y., Zhou, L., Jiang, B., Op Den Camp, H.J.M., Risgaard-Petersen, N., Schwark, L., Peng, Y., Hefting, M.M., Jetten, M.S.M., Yin, C., 2013. Hotspots of anaerobic ammonium oxidation at land-freshwater interfaces. Nat. Geosci. 6: 103–107. https://doi.org/10.1038/ngeo1683.